J. Fluid Mech. (1983), *vol.* 133, *pp.* 1–16
Printed in Great Britain

Flow in alluvial-river curves

By MARCO FALCÓN ASCANIO
Instituto de Mecanica de Fluidos, Facultad de Ingenieria, Universidad Central de Venezuela, Caracas, Venezuela

AND JOHN F. KENNEDY
Institute of Hydraulic Research, The University of Iowa, Iowa City, U.S.A.

(Received 8 September 1982)

Uniform flow in curved, wide, erodible-bed channels is formulated on the basis of the conservation of flux of moment-of-momentum, to obtain relations for the vertical distributions of radial-plane velocity and radial shear stress. The expression for the radial stress exerted on the bed is utilized in a force-equilibrium analysis of the moving bed layer to obtain relations for the average transverse slope of the bed and for the radial bed profile. The reduction of primary bed shear stress due to the net radial transport of streamwise momentum toward the outer (concave) bank is then calculated, by introducing the derived expressions for the velocity components into the momentum equation for the primary-flow direction. It is found that the stress reductions in deep, narrow channels can exceed 50%. Bed profiles and velocity distributions measured in natural and laboratory streams are found to be in good conformity with those calculated from this moment-based theory.

1. Introduction

Even casual observers of Earth's geological features soon notice that natural alluvial streams are seldom straight along reaches of more than a few channel widths. Hydraulic engineers and other students of fluvial processes have long recognized meandering to be not only an intriguing geometrical and kinematical feature of rivers, but also one that has major effects on their sediment-transport and roughness characteristics. Fluid mechanicians appreciate further that the internal structure of flow in meandering rivers is as fascinating as their migrating, serpentine channel lineament. Especially engaging is the interaction between the vertical profile of the primary flow and the centrifugal forces resulting from the flow's curvature. The principal result is the well-known spiralling or secondary flow in planes normal to the channel axis. Because the bed-surface sediment of a stream actively transporting its bed material is in a quasifluidized state, even the relatively small radial component of the bed shear stress and small near-bed velocities produced by the secondary flow transport sediment toward the inner (convex) banks until the bed becomes inclined such that the gravity and shear forces exerted radially along the bed on the moving bed-load particles are in balance. The resulting greater depth near the outer banks increases the primary-flow velocities there, which in turn intensifies the erosive attack on the banks and also undermines them. Both of these effects aggravate bank erosion and thereby promote further growth of the meanders.

Although the seemingly disproportionate effects of channel meandering on river flow have been appreciated for several decades, attempts to develop a mathematical

model for the secondary flow and its interactions with the primary flow and sediment motion have met with only limited success. The principal stumbling block encountered arises from the radial shear-stress force exerted on an elemental control volume at any elevation (the vertical distribution of which is the principal determinant of the radial-plane velocity profile) being the small difference between two much larger quantities: the centrifugal body force and the radial pressure force resulting from superelevation of the water surface. It is important to bear in mind that even though the integrals of these two forces over the depth are very nearly equal, locally they are grossly out of balance. The radial gradient of pressure resulting from the transverse inclination of the free surface is very nearly constant over the depth, while the centrifugal force varies from zero at bed level to a maximum near the free surface. In fact, it is precisely the difference between the distributions of these two nearly equal forces that is responsible for the secondary flow. Moreover, the secondary flow (or, viewed differently, the vertical gradient of the primary velocity) causes the radial water-surface slope to be greater than it would be for a flow with vertically uniform primary velocity (which would not produce a secondary current). This is because the secondary flow produces an inward radial shear force on the bed; the corresponding radially outward force on the flow must be balanced by part of the radial pressure-gradient force. Thus, just in determining the distributions of the three principal radial forces – pressure, shear and centrifugal – exerted on the flow, one is faced with the problem of having two of them – shear and pressure – unknown, even if the velocity distribution of the primary flow and hence also the centrifugal-force distribution are known. Clearly, to proceed with the calculation of these forces, another relation, in addition to the equation expressing the balance of radial forces, is needed. Further physical considerations or assumptions must be introduced to calculate the distribution of the radial velocity.

In the analytical model developed here for vertical distributions of radial shear stress and velocity, and radial distributions of depth and streamwise velocity, an expression for the conservation of moment-of-momentum is the additional relation utilized to close the formulation of the radial forces. This aspect of the analysis is similar, for example, to use of equations expressing balances of forces and moments to calculate the supporting forces on a loaded, simply supported beam. One of the two unknown forces does not appear in the formulation of moments about one of the supports, and therefore the other can be calculated directly. A roughly parallel approach is followed in the present analysis. Formulation of the flux of moment-of-momentum about the longitudinal axis at the bed surface yields an expression for the radial pressure gradient. The radial momentum equation then is used to obtain the vertical distribution of radial shear stress. The transverse bed profile is determined from consideration of the force balance for the moving bed-load particles. The radial-velocity profile is calculated by introducing into the radial momentum equation a linear primary-shear-stress distribution and the eddy-viscosity distribution obtained from the power-law distribution utilized for the primary velocity. Finally, the radial distribution of local depth corresponding to the bed profile is used in the calculation of the transverse distribution of depth-averaged streamwise velocity. The analysis is limited to a channel of constant centreline radius, which is a good approximation to extended reaches of bows of many strongly meandering natural channels. Extension of the analytical model to weakly meandering channels is developed in Falcón Ascanio's (1979) thesis.

Some of the background literature on this problem is cited in connection with development of the present model. For a more complete review, reference is made

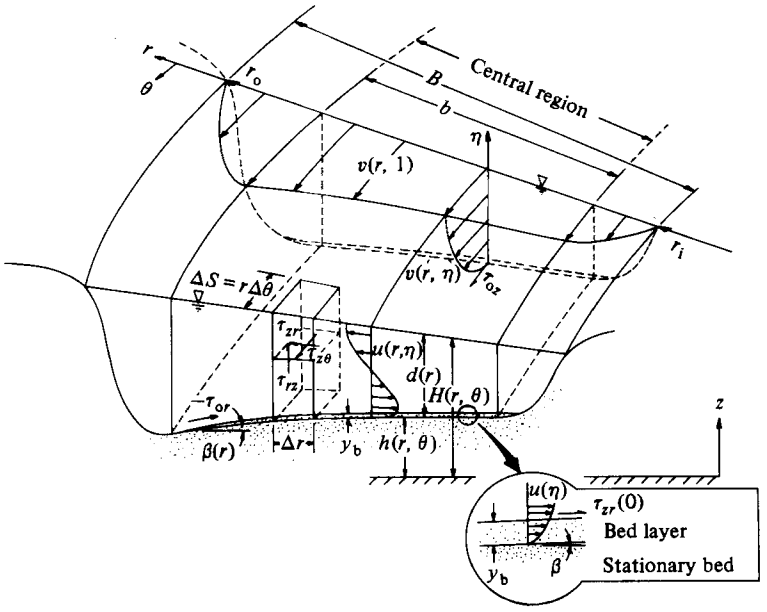

FIGURE 1. Definition sketch for flow in an alluvial-channel bend.

to the surveys by Callander (1968, 1978), to Falcón Ascanio's (1979) thesis, and to Odgaard's (1981) paper on river-bend topography.

2. Analysis

2.1. *General*

The idealized channel treated here has infinite length, constant width, an erodible sediment bed, and banks with a common centre of curvature. The central, longitudinal channel axis at the level of the bed has constant mean slope S_c, and describes a helix in space which traces a circle of radius r_c when projected onto a horizontal plane. The flow is conveniently described in cylindrical coordinates: the vertical z-axis passes through the curvature centre of the channel and is positive in the direction opposite to gravity; in planes perpendicular to the z-axis, locations are specified by radial distance r from the z-axis, and polar angle θ, as shown in figure 1. In order for the radial slopes of the bed and water surface to be constant along the channel, the local streamwise slope $S(r)$ of both must be

$$S = S_c \frac{r_c}{r}. \tag{1}$$

The flow is treated as uniform in the sense that its properties are invariant along any helix with constant radius r and slope S. The analysis will be restricted further to a central region of the channel, delineated in figure 1, throughout which the vertical velocity is much smaller than the characteristic velocities in the r- and θ-directions. The channel slope S_c will be limited to small values, so that forces and velocities parallel to the underlying bed-surface helices may be taken to be equal to those along the θ-coordinate. Finally, the restriction $d/r \ll 1$ will be imposed, for reasons that become apparent in the next section.

2.2. *Vertical distribution of radial shear stress*

Calculation of the radial shear stress at any elevation requires, first, that the radial water-surface slope and associated pressure gradient be determined, for use in calculation of the vertical distribution of radial shear stress from the radial momentum equation. The radial water-surface slope will be calculated from a formulation, simplified by means of an ordering analysis, of the conservation of flux of moment-of-momentum for the control volume shown in figure 1, which extends over the whole flow depth and has base dimensions Δr and $\Delta s = r\Delta\theta$. For this control volume, the equation of moment-of-momentum about an axis r = constant at the bed surface is

$$d\int_0^1 \frac{\partial p}{\partial r}\eta\,\mathrm{d}\eta - d\int_0^1 \rho\frac{v^2}{r}\eta\,\mathrm{d}\eta + \int_0^1 \tau_{rz}\,\mathrm{d}\eta + \frac{1}{d}\frac{\partial}{\partial s}\left[d^2\int_0^1 \rho uv\eta\,\mathrm{d}\eta\right] + \frac{1}{rd}\frac{\partial}{\partial r}\left[rd^2\int_0^1 \rho u^2\eta\,\mathrm{d}\eta\right] - \int_0^1 \rho uw\,\mathrm{d}\eta = 0, \quad (2)$$

where, in addition to the quantities defined in figure 1, p = pressure, $\eta = (z-h)/d$, ρ = fluid density, $u(r,\eta)$, $v(r,\eta)$ and $w(r,\eta)$ = velocities in r-, θ- and z-directions respectively, and $\tau_{rz}(r,\eta) = \tau_{zr}(r,\eta)$ = shear stress acting on surfaces normal to r- and z-axes respectively. The fourth term in (2) is zero for uniform flow. The remaining terms will be ordered by taking $v = O(V)$, where $V(r)$ = depth-averaged flow velocity, $u = O(u(r,1) \equiv U_\mathrm{m})$, and the z-direction velocity $w = O(w_{\max} \equiv W_\mathrm{m})$. Relative to the second term, the fifth and sixth terms are $O(U_\mathrm{m}^2/V^2)$ and $O((r/d)\,(U_\mathrm{m}/V)\,(W_\mathrm{m}/V))$ respectively. Yen (1965) concluded from his measurements of flow in curved channels that $U_\mathrm{m}/V = O(d/r)$. This result is suggested also by the analysis of Zimmermann & Kennedy (1978, equation (7)), which shows the ratio of radial to streamwise components of bed shear stress to be $O(d/r)$. If $z = O(d)$, the continuity equation

$$\frac{u}{r} + \frac{\partial u}{\partial r} + \frac{\partial v}{\partial s} + \frac{\partial w}{\partial z} = 0, \quad (3)$$

in which $\partial v/\partial s$ is zero for the uniform flow being considered, requires that $W_\mathrm{m}/U = O(d/r)$. Because $U_\mathrm{m}/V = O(d/r)$, it follows that $W_\mathrm{m}/V = O(d/r)^2$. It is concluded then that the fifth and sixth terms of (2) are both $O(d/r)$ relative to the centrifugal-force (second) term, and can be dropped.

The shear-stress (third) term of (2) may be ordered by utilizing the equality of shear stresses and the Boussinesq shear-stress relation for turbulent flow, and treating the eddy viscosity ϵ_0 as constant over the depth:

$$\int_0^1 \tau_{rz}\,\mathrm{d}\eta = \int_0^1 \tau_{zr}\,\mathrm{d}\eta = \rho\frac{\epsilon_0}{d}\int_0^1 \frac{\partial u}{\partial \eta}\,\mathrm{d}\eta = \rho\frac{\epsilon_0 U_\mathrm{m}}{d}. \quad (4)$$

The eddy viscosity may be expressed as a product of the shear velocity u^* and depth; therefore

$$\int_0^1 \tau_{rz}\,\mathrm{d}\eta = O(\alpha\rho u_* U), \quad (5)$$

where $\alpha \approx \epsilon_0/u_* d$ ($\alpha = 0.079$, according to Hinze 1975). From (5) it follows that

$$\frac{\int_0^1 \tau_{rz}\,\mathrm{d}\eta}{d\int_0^1 \rho\frac{v^2}{r}\eta\,\mathrm{d}\eta} = O\left(\alpha\frac{r}{d}\frac{u_*}{V}\frac{U}{V}\right) = O(\alpha(\tfrac{1}{8}f)^{\frac{1}{2}}), \quad (6)$$

in which f = Darcy–Weisbach friction factor. Both α and $(\frac{1}{8}f)^{\frac{1}{2}}$ are $O(10^{-1})$, and therefore the third term of (2) is two orders of magnitude smaller than the second and may be disregarded. Because $p = O(\rho V^2)$, the first and second terms are of the same order. Incorporation of the simplifications resulting from the foregoing ordering analysis reduces (2) to

$$\int_0^1 \frac{\partial p}{\partial r}\eta\,\mathrm{d}\eta = \rho\int_0^1 \frac{v^2}{r}\eta\,\mathrm{d}\eta. \tag{7}$$

In the central region, where $U_m/V \ll 1$ and $W_m/V \ll 1$, it is reasonable to assume that the vertical distribution of p is hydrostatic:

$$\frac{\partial p}{\partial r} = \rho g\frac{\partial H}{\partial r} \equiv \rho g H', \tag{8}$$

where g = gravitational acceleration and H is defined in figure 1. It has been demonstrated by Yen (1965) that the deviation of the pressure from the hydrostatic distribution is $O(d/r)$ or smaller in even moderately curved open-channel flow. The primary-flow velocity $v(r,\eta)$ will be expressed by the power law

$$\frac{v}{V} = \frac{n+1}{n}\eta^{1/n}, \tag{9}$$

where $1/n$ is an exponent which is related to the Darcy–Weisbach friction factor by

$$\frac{1}{n} = \frac{1}{\kappa}(\tfrac{1}{8}f)^{\frac{1}{2}}, \tag{10}$$

where κ = von Kármán's constant. The background of this relation is reviewed by Zimmermann & Kennedy (1978). Karim (1981) examined (10) critically, verified it with laboratory data, and formulated the dependence of κ on sediment concentration; this refinement will not be included in the present analysis. Substitution of (8) and (9) into (7) yields

$$H'(r) = \frac{n+1}{n}\frac{V^2}{rg}. \tag{11}$$

By means of an ordering analysis similar to the one developed above and guided in some measure by his experimental results, Yen (1965) simplified the radial momentum equation for curved open-channel flow to

$$gH' - \frac{v^2}{r} - \frac{1}{\rho d}\frac{\partial \tau_{zr}}{\partial \eta} = 0. \tag{12}$$

It is noteworthy that τ_{zr} makes a first-order contribution to the radial-momentum relation, but the corresponding vertical shear stress τ_{rz} makes only a higher-order contribution to the moment-of-momentum equation if the moment axis is taken at bed level to avoid inclusion of the bed shear stress. This is, in fact, the motivation for utilizing the moment relation: it avoids specification of τ_{rz} at the bed in the determination of H'. Substitution of (9) into (12), integration of the resulting expression from arbitrary η to $\eta = 1$, and application of the boundary condition $\tau_{rz}(1) = 0$ yields

$$\tau_{zr}(r,\eta) = \rho g d\left[H'(\eta-1) - \frac{V^2}{rg}\frac{(n+1)^2}{n(n+2)}(\eta^{(2+n)/n}-1)\right]. \tag{13}$$

2.3. *Transverse bed profile and depth distribution*

Equilibrium of the transverse bed profile, $h(r, \theta)$ in figure 1, and of the depth $d(r)$ are attained when the radial-plane forces acting on the moving bed-load particles sum to zero. Bed-load movement will be treated as occurring in a layer of thickness y_b, as shown in figure 1. The shear forces exerted on this agitated, somewhat-dilated, moving layer are in reality diffuse 'seepage' forces caused by the flow within the layer's interstices, and any net force, however small, in the radial direction will produce transverse motion of the bed-load particles. Therefore, radial equilibrium will be reached when the local bed inclination $\beta(r)$ is such that

$$\tau_{0r} = \tau_{zr}(r, 0) = y_b(1-p)\,\Delta\rho\, g \sin\beta, \tag{14}$$

where p = porosity of the bed-layer; $\Delta\rho = \rho_s - \rho$; and ρ_s = density of bed particles. In the development of his detailed, computer-simulation model of sediment transport in streams, Karim (1981) concluded from inferential evidence that

$$y_b = D_{50}\frac{u_*}{u_{*c}}, \tag{15}$$

where D_{50} = median bed-material size; $u_*(r)$ = local shear velocity = $V(\frac{1}{8}f)^{\frac{1}{2}}$; and u_{*c} = critical shear velocity for incipient particle motion. In terms of the Shields parameter θ, u_{*c} may be expressed as

$$u_{*c} = \left(g\frac{\Delta\rho}{\rho}D_{50}\theta\right)^{\frac{1}{2}}, \tag{16}$$

which defines θ. Substitution of (13), (11), (15) and (16) into (14), and incorporation of the simplification of (10) to Nunner's (1956) relation (Hinze 1975)

$$n = f^{-\frac{1}{2}}, \tag{17}$$

which corresponds to $\kappa = 0.354$, yields

$$S_T \equiv \sin\beta = \frac{d}{r}F_D\frac{(8\theta)^{\frac{1}{2}}}{1-p}\frac{1+f^{\frac{1}{2}}}{1+2f^{\frac{1}{2}}}, \tag{18}$$

where

$$F_D = \frac{V}{(g(\Delta\rho/\rho)\,D_{50})^{\frac{1}{2}}}.$$

The traverse bed profile may be calculated by neglecting the effect of H' on $d(r)$; then

$$\sin\beta = \frac{\mathrm{d}d}{\mathrm{d}r}. \tag{19}$$

The velocity V to be used in (18) is obtained by incorporating (1) into the local expression of the Darcy–Weisbach friction factor:

$$V(r) = \left(8\frac{\tau_{0\theta}}{\rho f}\right)^{\frac{1}{2}} = \left(8\frac{\delta S\rho g d(r)}{\rho f}\right)^{\frac{1}{2}} = \left(8S_c\frac{r_c}{r}\frac{g\delta d(r)}{f}\right)^{\frac{1}{2}}, \tag{20}$$

where $\tau_{0\theta}$ = longitudinal shear stress acting on the bed, and $\delta(r)$ = bed-shear-stress reduction factor defined by

$$\tau_{0\theta}(r) = \delta S\rho g d(r), \tag{21}$$

which takes into account the transport of primary-flow momentum out of the central region to the vicinity of the outer bank, where it is balanced by bank shear. An analysis of δ is developed in §2.6. Substitution of (19), (20) and (1) into (18) and

integration of the resulting expression for $\mathrm{d}d/\mathrm{d}r$ yields

$$\frac{1}{d^{\frac{1}{2}}} - \frac{1}{d_c^{\frac{1}{2}}} = \left[\frac{1}{r^{\frac{1}{2}}} - \frac{1}{r_c^{\frac{1}{2}}}\right] \frac{(8\theta)^{\frac{1}{2}}}{1-p} \frac{1+f^{\frac{1}{2}}}{1+2f^{\frac{1}{2}}} \left(\frac{8S_c r_c g\delta}{fg\dfrac{\Delta\rho}{\rho} D_{50}}\right)^{\frac{1}{2}}, \tag{22}$$

where the subscript c denotes the centreline values used in setting the integration constant. Elimination of δS_c from (22) by means of (20) and replacing V by its section-averaged value $\overline{V}$ for the whole flow, to facilitate verification, leads to

$$\left(\frac{d}{d_c}\right)^{\frac{1}{2}} = 1 - \left[1 - \left(\frac{r}{r_c}\right)^{\frac{1}{2}}\right] \frac{(8\theta)^{\frac{1}{2}}}{1-p} \frac{1+f^{\frac{1}{2}}}{1+2f^{\frac{1}{2}}} \overline{F}_D, \tag{23}$$

where

$$\overline{F}_D = \frac{\overline{V}}{g(\Delta\rho/\rho) D_{50})^{\frac{1}{2}}}.$$

Utilization of the mean velocity for the whole cross-section in the calculation of $d(r)$ from (23), or in calculating an average value of S_T from (18) by replacing F_D with F_D, neglects the effects of the variation of V across the channel, but nevertheless yields satisfactory results, as is demonstrated in §3.

Equations (20) and (23) give the radial distribution of mean velocity for uniform flow. In practical applications, it generally suffices to take $\delta = 1$.

2.4. *Vertical distribution of transverse velocity*

Calculation of the radial-plane velocity will incorporate the following assumptions.

(i) The primary-flow shear stress $\tau_{z\theta}$ is linearly distributed, and $\partial\tau_{r\theta}/\partial r$ makes a negligible contribution to the streamwise force balance:

$$\tau_{z\theta}(r, \eta) = \tau_{0\theta}(1-\eta) = \delta\rho g d S(1-\eta). \tag{24}$$

(ii) The eddy viscosity is isotropic and is given by

$$\epsilon(r, \eta) = \frac{d\tau_{z\theta}}{\rho\,\partial v/\partial\eta}. \tag{25}$$

(iii) Because of the isotropy of ϵ, the radial velocity and shear stress are related by

$$\tau_{zr}(r, \eta) = \frac{\rho\epsilon}{d}\frac{\partial u}{\partial\eta}. \tag{26}$$

Substitution of (9) and (24) into (25) yields

$$\epsilon = \frac{\delta g d^2 S_c r_c}{rV} \frac{n^2}{n+1} (1-\eta)\,\eta^{(n-1)/n}, \tag{27}$$

which, when substituted along with (13) into (26), leads to

$$\frac{u}{V} = \frac{1}{\delta S_c}\frac{r}{r_c}\frac{n+1}{n^2}\int_0^\eta \left[-H'\eta^{(1-n)/n} - \frac{V^2}{rg}\frac{(n+1)^2}{n(n+2)}\frac{\eta^{3/n} - \eta^{(1-n)/n}}{1-\eta}\mathrm{d}\eta\right]. \tag{28}$$

For steady uniform flow, u must satisfy

$$\int_0^1 u(\eta)\,\mathrm{d}\eta = 0. \tag{29}$$

There is no assurance that (28) will satisfy this requirement if H' given by (11) is utilized, because of errors inherent in the Boussinesq eddy-viscosity model and other

assumptions that have been made in the derivation of the relation for u. Therefore the integral of (29) will be evaluated for arbitrary H', denoted by H'_u and expressed as

$$H'_u(r) \equiv T\frac{n+1}{n}\frac{V^2}{rg}, \tag{30}$$

where $T = H'_u/H'$, and H' is given by (11). Substitution of (28) and (30) into (29), utilization of the expansion

$$\frac{1}{1-\eta} = \sum_{j=0}^{\infty} \eta^j, \quad \eta < 1, \tag{31}$$

and term-by-term integration of the resulting series yields

$$\frac{u}{V} = \frac{1}{\delta S_c}\frac{V^2}{gr_c}\left(\frac{n+1}{n}\right)^3\left[-T\eta^{1/n} - \frac{1}{n+2}\sum_{j=0}^{\infty}\left(\frac{\eta^{3/n+1+j}}{3/n+1+j} - \frac{\eta^{1/n+j}}{1/n+j}\right)\right]. \tag{32}$$

Equation (29) is satisfied if T is given by

$$T(n) = -\frac{n+1}{n^2(n+2)}\sum_{j=0}^{\infty}\left[\frac{1}{(3/n+2+j)(3/n+1+j)} - \frac{1}{(1/n+1+j)(1/n+j)}\right]. \tag{33}$$

Incorporation of (17), (20) and (33) into (32) gives

$$\begin{aligned}\frac{u}{V}\frac{r}{d} &= 8\sum_{j=0}^{\infty}\left\{\frac{(n+1)^4}{n^2(n+2)}\left[\frac{1}{(3/n+2+j)(3/n+1+j)} - \frac{1}{(1/n+1+j)(1/n+j)}\right]\eta^{1/n}\right.\\ &\quad\left. - \frac{(n+1)^3}{n(n+2)}\left[\frac{\eta^{3/n+1+j}}{3/n+1+j} - \frac{\eta^{1/n+j}}{1/n+j}\right]\right\}\\ &\equiv G(\eta, n).\end{aligned} \tag{34}$$

Equation (34) is shown in figure 2 for four values of n which span the range from very rough ($n = 2.5, f = 0.16$) to relatively smooth ($n = 10, f = 0.01$) channels. It is noteworthy that, for all but very low values of n, the velocity profiles are nearly linear except near the bed, with $u = 0$ at about mid-depth.

2.5. *A remark on H' and H'_u*

In the foregoing analysis, two expressions were derived for the transverse slope of the water surface: (11), and (30) and (33). Corresponding to each of these is a different value of $\tau_{zr}(0)$, the radial component of the bed shear stress. Their ratio $T = H'_u/H'$ given by (33) has a nearly constant value of 0.9 for $2 < n < 8$. In view of the near equality of H'_u and H', why was it necessary to utilize different values in the formulations of τ_{zr} and of $u(\eta)$? The problem is one of sensitivity, as will now be demonstrated. Equation (13) gives

$$\tau_{0r}(r) \equiv \tau_{zr}(r, 0) = \rho g d\left[\frac{V^2}{rg}\frac{(n+1)^2}{n(n+2)} - H'\right], \tag{35}$$

which together with (11) for H' shows that τ_{0r} is the difference between two small quantities multiplied by a large one, $\rho g d$. Therefore small errors in the expression for the transverse water slope produce large errors in τ_{0r}. For example, the ratio of τ_{0r} given by (35) with H' replaced by H'_u obtained from (30) and (33), to τ_{0r} yielded by (35) and (11) varies widely with n, from about 0.6 for $n = 2$ to nearly 0.2 for $n = 8$. Because the radial bed slope and thus also the bed profile depend directly on τ_{0r}, as is shown by (14), it is important in their derivation to have an accurate estimate of τ_{0r} – one whose calculation avoids use of such artifices as the Boussinesq relation, and

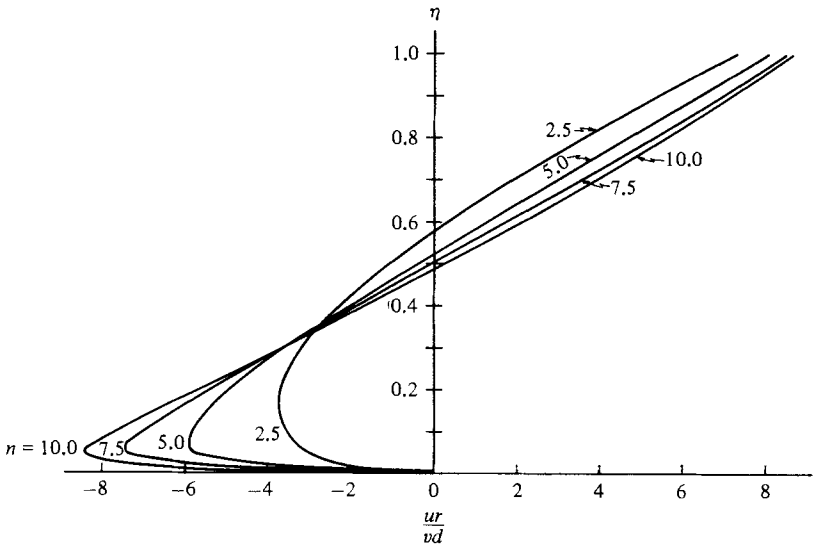

FIGURE 2. Distribution of radial-plane secondary-flow velocity given by (34).

instead directly utilizes a mechanics principle such as conservation of moment of momentum. The effect of the radial water-surface slope on $u(\eta)$ calculated from the Boussinesq relation may be examined by substituting (26) into (12) and treating ϵ as constant, say ϵ_0, which results in

$$\frac{\partial^2 u}{\partial \eta^2} = \frac{gd^2}{\epsilon_0}\left(\frac{v^2}{gr} - H'\right). \tag{36}$$

Equation (36) shows that $\partial^2 u/\partial\eta^2$, and hence $u(\eta)$, also is very sensitive to the small difference between two nearly equal quantities multiplied by a large one. Accordingly, only a very small adjustment in the radial water-surface slope is required to compensate for the effects on u of the assumptions made in its calculation, and thereby to permit u to satisfy the continuity requirement (29). But this small adjustment in H' – amounting to only about 10 %, as just noted – has a major effect on τ_{0r}, as (35) demonstrates.

2.6. *Secondary-flow effects on $\tau_{z\theta}$ and v*

In a laterally non-uniform curved flow, the secondary current produces a net radial transport of streamwise (θ-direction) momentum out of the central region, which in turn reduces $\tau_{z\theta}$, and in so doing modifies $v(r, \eta)$ (or n). It was anticipation of this effect which prompted incorporation of the factor $\delta(r)$ into the shear-stress expressions (20) and (21). Calculation of δ and the secondary-flow effect on $v(\eta)$ proceeds from the θ-direction momentum equation with $\tau_{r\theta}$ neglected,

$$u\frac{\partial v}{\partial r} + v\frac{\partial v}{\partial s} + w\frac{\partial v}{\partial z} + \frac{uv}{r} = -g\frac{\partial H}{\partial s} + \frac{1}{\rho}\frac{\partial \tau_{z\theta}}{\partial z}. \tag{37}$$

Multiplication of (3) by v, addition of the result to (37), integration of the new relation from η to 1, and imposition of the boundary condition $\tau_{z\theta}(r, 1, \theta) = 0$ gives

$$\tau_{z\theta} = \rho d\left[-\int_\eta^1 \frac{\partial(uv)}{\partial r}\,\mathrm{d}\eta - \frac{2}{r}\int_\eta^1 uv\,\mathrm{d}\eta - \int_\eta^1 \frac{\partial v^2}{\partial s}\,\mathrm{d}\eta - \frac{1}{d}[(wv)_{\eta=1} - wv] + gS(1-\eta)\right], \tag{38}$$

where $S = -\partial H/\partial s$. The z-velocity w is evaluated from the continuity equation, (3), the relation, for u, (32) and the identities

$$\frac{\partial \eta}{\partial r} = -\frac{-d\,\partial h/\partial r - (z-h)\,\partial d/\partial r}{d^2}$$

$$= \frac{-d\,\partial(H-d)/\partial r - \eta d\,\partial d/\partial r}{d^2}$$

$$= \frac{(1-\eta)\,\mathrm{d}d/\mathrm{d}r - \partial H/\partial r}{d}, \tag{39}$$

and, similarly,

$$\frac{\partial \eta}{\partial s} = \frac{S}{d}. \tag{40}$$

The result is

$$w(r,\eta) = -\left[\frac{d}{r} + \frac{\mathrm{d}d}{\mathrm{d}r} + d\left(\frac{3}{\bar{V}}\frac{\mathrm{d}V}{\mathrm{d}r} - \frac{1}{\delta}\frac{\mathrm{d}\delta}{\mathrm{d}r}\right)\right]\int_0^\eta u\,\mathrm{d}\eta + \left[\frac{\partial H}{\partial r} - \frac{\mathrm{d}d}{\mathrm{d}r}(1-\eta)\right]u - Sv. \tag{41}$$

Substitution of (9), (34) and (41) for v, u and w, along with

$$\frac{\partial v^2}{\partial s} = \frac{S}{d}\frac{\partial v^2}{\partial \eta} \tag{42}$$

into (38) yields

$$\frac{\tau_{z\theta}}{\rho g S D} = (1-\eta) - 64\delta\frac{d}{r}n(n+1)\left\{\left[\frac{\mathrm{d}d}{\mathrm{d}r} + 2\frac{d}{r} + 4\frac{d}{V}\frac{\mathrm{d}V}{\mathrm{d}r} - \frac{d}{\delta}\frac{\mathrm{d}\delta}{\mathrm{d}r}\right]\int_\eta^1 G(n,\eta)\,\eta^{1/n}\,\mathrm{d}\eta\right.$$

$$\left. + \left[\frac{\mathrm{d}d}{\mathrm{d}r} + \frac{d}{r} + 3\frac{d}{V}\frac{\mathrm{d}V}{\mathrm{d}r} - \frac{d}{\delta}\frac{\mathrm{d}\delta}{\mathrm{d}r}\right]\eta^{1/n}\int_0^\eta G(n,\eta)\,\mathrm{d}\eta\right\}, \tag{43}$$

where G is defined by (34).

The first term on the right-hand side of (43) is the linear shear-stress distribution, and the second term expresses the shear-stress reduction due to the transverse gradient of lateral flux of streamwise momentum. In the calculation of $\tau_{z\theta}$ it is assumed that the $\partial\delta/\partial r$ term is negligible in comparison with the other derivative terms in brackets. Substitution of (18) for $\mathrm{d}d/\mathrm{d}r$ and of (20) for V then permits calculation of the shear stress at any location. The bed-shear-stress reduction factor δ, introduced in (20) and (21), is obtained by letting $\eta = 0$ in (43). To gain some idea of its magnitude, a representative constant value of δ for the whole central region, say $\bar{\delta}$, will be determined. For this calculation it is appropriate to replace V and d by their section-averaged values $\bar{V}$ and $\bar{d}$, after carrying out the substitutions and taking the derivatives in (43); and to take $r = r_c$. The result is

$$\bar{\delta} = \frac{\tau_{0\theta}}{\rho g S \bar{d}} = \left[1 + 192\frac{\bar{d}}{r_c}n(n+1)\,\bar{S}_T\int_0^1 G(n,\eta)\,\eta^{1/n}\,\mathrm{d}\eta\right]^{-1}, \tag{44}$$

where $\bar{S}_T$ is obtained from (18) by replacing d and V by $\bar{d}$ and $\bar{V}$. The integral of (44) was evaluated numerically, with the result shown in figure 3. Values of $\bar{\delta}$ for some field and laboratory flows are presented in §3.

The effect of the secondary flow on the primary-flow velocity distribution may be estimated by substituting (17) into (20) and replacing δ by $\bar{\delta}$. If V is considered to be constant, η is increased, as $\delta^{-\frac{1}{2}}$, which corresponds to the velocity profile becoming blunter. This is the observed effect of seconday flow on $v(\eta)$ (Falcón Ascanio 1979).

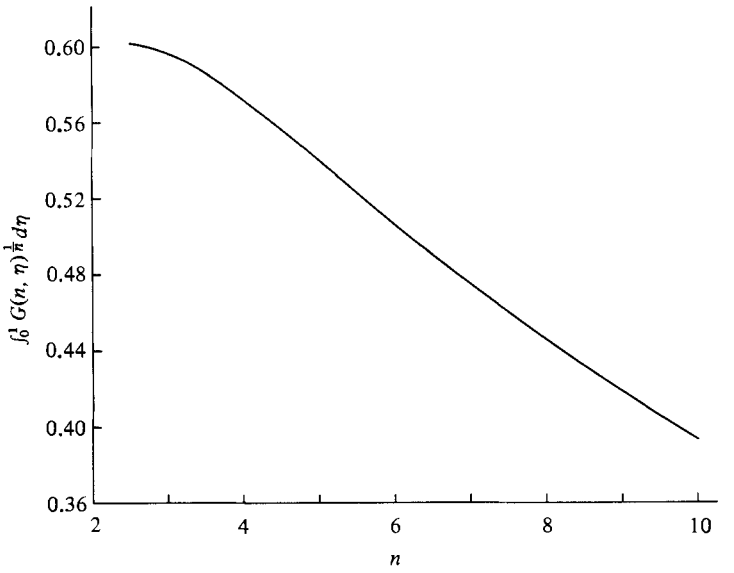

FIGURE 3. Result of the numerical evaluation of $\int_0^1 G(n,\eta)\,\eta^{1/n}\,\mathrm{d}\eta$, where G is given by (34).

3. Verification

Data utilized in the verifications reported here are summarized in table 1. Falcón Ascanio (1979) presents additional comparisons of measured and computed quantities.

3.1. *Bed topography*

Zimmermann (1974) and Zimmermann & Kennedy (1978) reported the results of experiments conducted in three concentric, 60 cm wide, circular-planform flumes with a central angle that approached 2π. Two different sediments, with median diameters of 0.21 mm and 0.55 mm, were used. Longitudinal bed profiles were measured at 11 different radii, and the transverse bed profiles obtained from them for numerous cross-sections in the reaches of fully developed flow were plotted and averaged. The transverse profiles were found to be slightly convex upward, as illustrated in figure 4. Mean transverse bed slopes, averaged across numerous sections for each run, were then computed. Figure 5 shows the transverse slopes $\bar{S}_T$ so determined, plotted in the format of (18) based on cross-section averaged flow properties and the bed-section friction factor (Vanoni 1975). Excellent agreement between measured and computed values is obtained if $(8\theta)^{\frac{1}{2}}/(1-p) = 1.3$. If the limiting value (for fully turbulent boundary layers) of the Shields parameter $\theta = 0.06$ is adopted, the resulting porosity is $p = 0.47$, a not-unreasonable value for the agitated, moving bedload particles. The computed profile for Zimmermann's (1974) run no RII-13 show in figure 4 was obtained from (23), using these values of θ and p. The centreline depth $d_c = 9.66$ cm utilized in computing the profile was obtained by equating the reported depth, 10.1 cm, to the mean depth $\bar{d}$ calculated by integration of d given by (23) across the channel width:

$$\frac{\bar{d}}{d_c} = 1-2\phi+2\phi^2+\frac{4}{3}\frac{(\phi-\phi^2)\,(r_0^{\frac{3}{2}}-r_i^{\frac{3}{2}})}{r_c^{\frac{1}{2}}(r_0-r_i)}, \tag{45}$$

where

$$\phi = \bar{F}_D\frac{(8\theta)^{\frac{1}{2}}}{1-p}\frac{1+f^{\frac{1}{2}}}{1+2f^{\frac{1}{2}}},$$

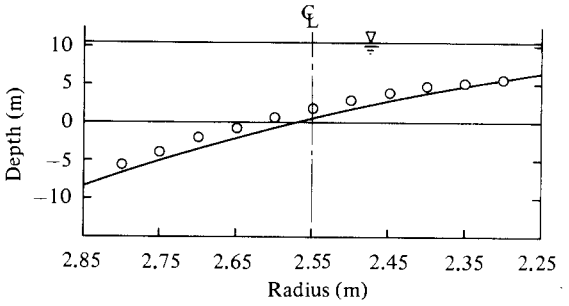

FIGURE 4. Transverse bed profiles measured in Zimmermann's (1974) run RII-13, and computed from (23).

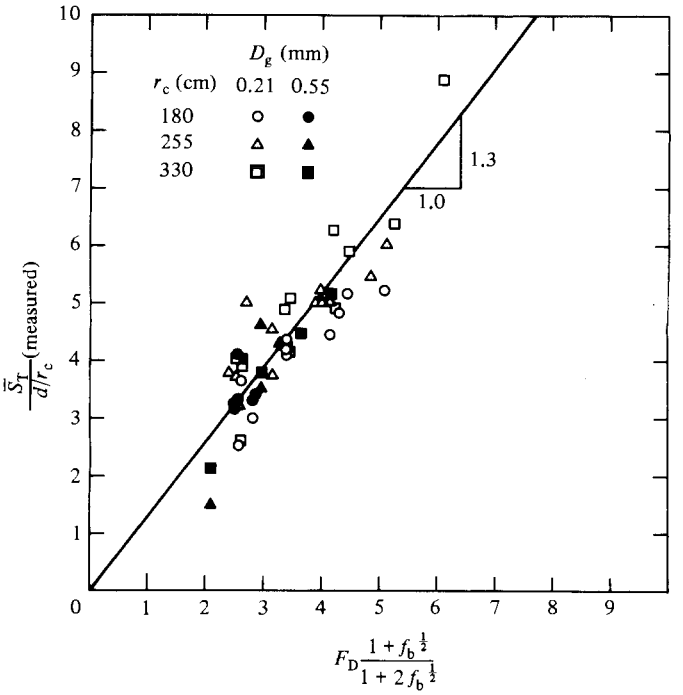

FIGURE 5. Comparison of (18) and Zimmerman & Kennedy's (1978) measured transverse bed slopes.

and r_i and r_o = radii of the inner and outer banks respectively. Calculation of the relation between $\bar{d}$ and d_c in this way is consistent with the measurement procedure that was used. Falcon (1978) describes calculation of $\bar{d}$ in a way that is consistent with conservation of bed-material volume in a curved channel. The friction factor utilized, $f_b = 0.165$ for this flow, is the value for the bed section obtained from the sidewall-correction procedure (Vanoni 1975, p. 152). The measured and computed profiles are in excellent agreement. The bed-shear-stress reduction factor obtained from (44) for this flow is $\bar{\delta} = 0.43$, which shows that in this relatively narrow channel the secondary current produced a major reduction in the bed shear.

Figure 6 compares measured and computed transverse bed profiles for a Missouri River section (Falcón Ascanio 1979). In computing the profile, $\bar{d}$ was taken to be equal to d_c, because of the difficulty of determining r_c for a wide natural stream, and of

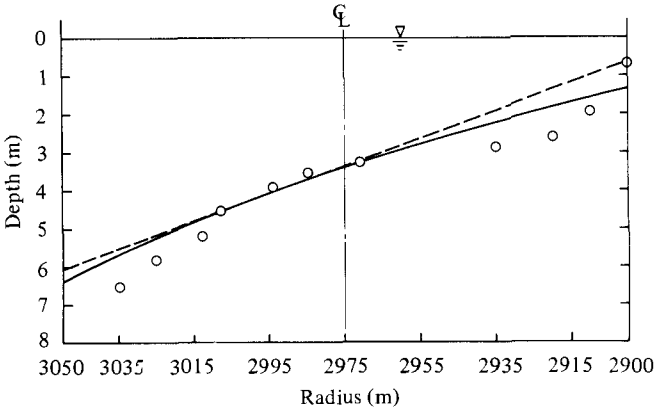

FIGURE 6. Transverse bed profile measured in Missouri River (Falcón Ascanio 1979), and those computed from (18) (----) and (23) (——).

the insensitivity of d_c to r_c (see (45)). Included in figure 6 is the mean bed profile given by (18), which also is seen to give quite good results. Equation (44) gives $\bar{\delta} = 0.97$ for this relatively wide, shallow flow, demonstrating the bed shear stress at any r in the central region of this natural channel is nearly equal to the local value of $\rho g d S$. Other comparisons of measured and computed bed profiles yielded conformities as good as those demonstrated in figures 4 and 6. In evaluating data from natural streams, in which the flow is seldom steady for appreciable periods, there is always uncertainty about the equilibrium of the bed topography. Moreover, the bed-material size often varies widely across a section, often by a factor of five or more. In view of these difficulties, it is suggested that, in the calculation of bed topography by means of (18) and (23), averaged (across channel sections, and along subreaches that are sufficiently short that r_c is practically constant) values of $\bar{d}$ and $\overline{V}$ be used, and that the median diameter of the material that can be moved by the flow be utilized for D_{50}. Furthermore, for most natural-stream situations, the refinement given by (23) is probably not justified; a straight-line profile with slope S_1 given by (18) and passing through $d = \bar{d}$ at $r = r_c$ is generally as accurate as the field data warrant, and perhaps within the reproducibility of bed topography of natural streams with their vagaries of discharge and bed-sediment characteristics.

3.2. *Velocity distributions*

It is very difficult to obtain reliable data on $u(\eta, r)$ in erodible-bed channels, because of the small values of the secondary-flow velocities, and of the problems posed by the moving sediment and the continuous bed changes attendant to migration of bed forms. Therefore the two measured profiles obtained by Kikkawa, Ikeda & Kitagawa (1976) from uniform flow in a circular-planform rigid channel were utilized in the verification of (34), with the results shown in figure 7. Kikkawa *et al.* developed an analytic model for $u(\eta)$, which can be seen in their paper also to yield generally satisfactory results except near the bed, where it does not satisfy the no-slip condition. Comparisons presented by Falcón Ascanio (1979) of (34) with the rigid, sinuous-channel data on transverse-velocities reported by Yen (1965) also demonstrate very satisfactory agreement.

Transverse distributions of V, the depth-averaged streamwise velocity, in erodible-bed channels are somewhat easier to measure than radial-velocity distributions. Velocity data obtained by Onishi (1972) at the apex cross sections in two of his

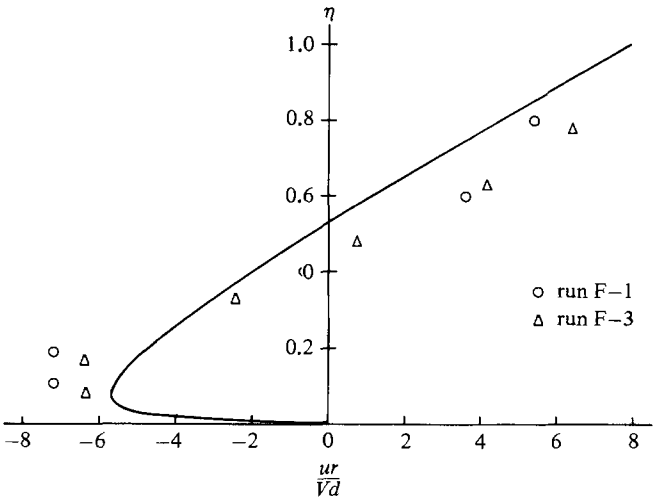

FIGURE 7. Secondary-flow velocity profiles measured by Kikkawa *et al.* (1976) and computed from (34).

rigid-bank erodible-bed meandering-channel flows were used to validate the distribution of V obtained from (20) and (23). The average friction factors $\bar{f}$ used in the computations were obtained from the reported mean values of velocity, depth and slope for the flows, and the Darcy–Weisbach relation in the form

$$\bar{f} = \frac{8g\bar{d}S}{\bar{V}^2}. \tag{46}$$

Note that computation of $\bar{f}$ from (46), which assumes $\delta = 1$, and of the corresponding n from (17), computation of $\bar{\delta}$ from (44) for this n, and use of $\bar{\delta}$ and $\bar{f}$ in (20) to determine $V(r)$ is slightly inconsistent. Falcón Ascanio (1979) recommends iteration between (20) with $V = \bar{V}$, (44) and (17) to obtain consistent values of n, f and $\bar{\delta}$. However, the convergence is quite rapid, and the effects on the computed $V(r)$ and $u(\eta)$ are not great. The computed and measured distributions of $V(r)$ shown in figure 8 agree quite well except near the banks, where V must tend to zero.

4. Concluding remarks

It must be borne in mind that the model developed here is strictly valid only for uniform, curved-channel flows. However, the available experimental data on flows in strongly curved channels (Zimmermann 1974; Zimmermann & Kennedy 1978; Odgaard & Kennedy 1982) indicate that they are characterized by relatively small phase shifts or lag distances between local secondary-flow properties or bed topography and local channel curvature. Therefore application of the present model utilizing local channel and flow characteristics in non-uniform flows, as was done in the foregoing comparison with Onishi's (1972) data, will generally yield satisfactory results. However, in the case of flow in weakly meandering sinuous channels, as investigated by Gottlieb (1976) and Falcón Ascanio (1979), the phase shift between local channel curvature and secondary-flow strength approaches $\frac{1}{2}\pi$.

The analytical model developed here is valid only for the central regions of curved-channel flows, which generally extend to about one local depth from the bank. In the near-bank regions, the flow becomes strongly three-dimensional and heavily

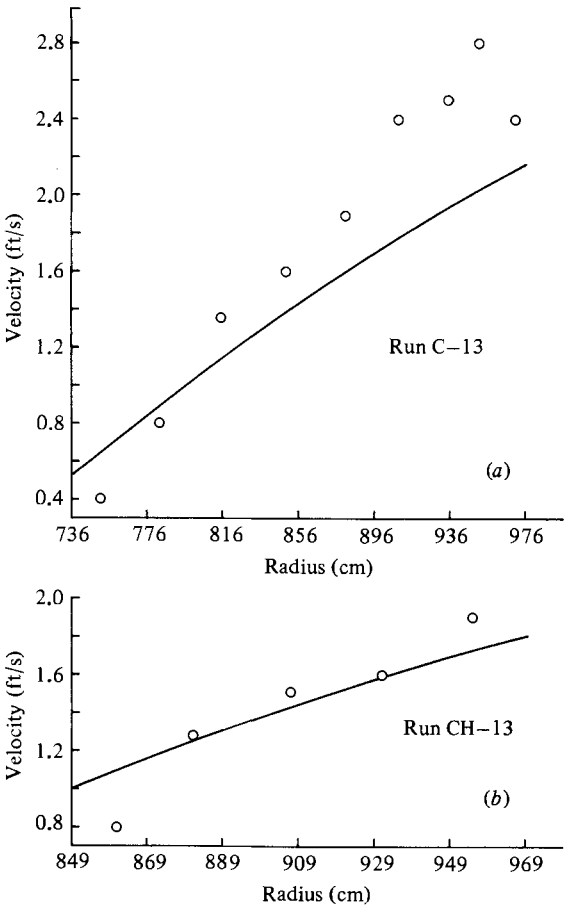

FIGURE 8. Comparison of Onishi's (1972) measured transverse distributions of depth-averaged velocity and those computed from (20) and (23).

influenced by local bank characteristics (erodibility, slope, roughness, etc.). Analysis of the flow and sediment transport in these regions is correspondingly more difficult than for the central region, and likely must await availability of better experimental data for its guidance.

The analysis presented here was largely developed in the course of the Ph.D. thesis research of the first author. Further work was done after his departure from The University of Iowa under the sponsorship of the U.S. Army Corps of Engineers Waterways Experiment Station (Contract DACW-39-80-C-0129). The analysis was completed and the manuscript prepared under support provided by the National Science Foundation (Grant CEE-8023003).

REFERENCES

CALLANDER, R. A. 1968 Instability and river meanders. Ph.D. thesis, University of Auckland, New Zealand.

CALLANDER, R. A. 1978 River meandering. *Ann. Rev. Fluid Mech.* **10**, 129–158.

FALCÓN ASCANIO, M. 1979 Analysis of flow in alluvial channel bends. Ph.D. Thesis, Dept. Mech. and Hydraul., University of Iowa.

GOTTLIEB, L. 1976 Three-dimensional flow pattern and bed topography in meandering channels. *Series Paper* 11, *Inst. Hydrodyn. and Hydraul. Engng, Tech. Univ. Denmark, Lyngby.*

HINZE, J. O. 1975 *Turbulence*, 2nd edn. McGraw-Hill.

KARIM, M. F. 1981 Computer-based predictors for sediment discharge and friction factor of alluvial streams. Ph.D. thesis, Dept Mech. and Hydraul., University of Iowa.

KIKKAWA, H., IKEDA, S. & KITAGAWA, A. 1976 Flow and bed topography in curved open channels. *J. Hydraul. Div. ASCE* **102** (HY9), 1327–1342.

NUNNER, W. 1956 Wärmeübergang und Druckabfall in rauhen Rohren. *VDI-Forschungscheft* 455, B, Band 2.

ODGAARD, A. J. 1981 Transverse bed slope in alluvial channel bends. *J. Hydraul. Div. ASCE* **107** (HY12), 1677–1694.

ODGAARD, A. J. & KENNEDY, J. F. 1982 Analysis of Sacramento River bend flows, and development of a new method for bank protection. *IIHR Rep.* no. 241, *Iowa Inst. Hydraul. Res., University of Iowa.*

ONISHI, Y. 1972 Effect of meandering on sediment discharges and friction factors of alluvial streams. Ph.D. thesis, Dept of Mech. and Hydraul., University of Iowa.

VANONI, V. A. (ed.). 1975 *Sedimentation Engineering.* Am. Soc. Civ. Engrs, Manual no. 54.

YEN, B. C. 1965 Characteristics of subcritical flow in a meandering channel. Ph.D. thesis, Dept. Mech. and Hydraul., University of Iowa. (Also available as unnumbered report from the Iowa Institute of Hydraulic Research.)

ZIMMERMANN, C. 1974 Sohlausbildung, Reibungsfaktoren, und sedimenttransport in gleichförmig gekrümmten und geraden Gerinnen. Ph.D. thesis, Inst. Hydromech. University of Karlsruhe.

ZIMMERMANN, C. & KENNEDY, J. F. 1978 Transverse bed slopes in curved alluvial streams. *J. Hydraul. Div. ASCE* **104** (HY1), 33–48.